The Spread of an Advantageous Allele Across a Barrier: The Effects of Random Drift and Selection Against Heterozygotes

Jaroslav Piálek*,† and Nick H. Barton*

**Institute of Cell, Animal, and Population Biology, University of Edinburgh, Edinburgh EH9 3JT, United Kingdom and †Academy of Sciences of the Czech Republic, Institute of Animal Physiology and Genetics, CZ-675 02 Studenec 122, Czech Republic*

Manuscript received December 19, 1995
Accepted for publication October 16, 1996

ABSTRACT

A local barrier to gene flow will delay the spread of an advantageous allele. Exact calculations for the deterministic case show that an allele that is favorable when rare is delayed very little even by a strong barrier: its spread is slowed by a time proportional to $\log((B/\sigma)\sqrt{2S})/S$, where B is the barrier strength, σ the dispersal range, and fitnesses are $1{:}1 + S{:}1 + 2S$. However, when there is selection against heterozygotes, such that the allele cannot increase from low frequency, a barrier can cause a much greater delay. If gene flow is reduced below a critical value, spread is entirely prevented. Stochastic simulations show that with additive selection, random drift slows down the spread of the allele, below the deterministic speed of $\sigma\sqrt{2S}$. The delay to the advance of an advantageous allele caused by a strong barrier can be substantially increased by random drift and increases with $B/(2S\rho\sigma^2)$ in a one-dimensional habitat of density ρ. However, with selection against heterozygotes, drift can facilitate the spread and can free an allele that would otherwise be trapped indefinitely by a strong barrier. We discuss the implications of these results for the evolution of chromosome rearrangements.

IN a spatially structured population, adaptation depends on the spread of genes throughout the region in which they are favored. If the species is sufficiently abundant that any particular mutation occurs frequently, or if selection acts on abundant polygenic variation, then adaptation will not be much slowed by spatial subdivision. However, in less numerous species, or where alleles are favored only in scattered habitats, lack of gene flow may limit the availability of the necessary variants. Even if the population does adapt rapidly, this adaptation may be based on different genes in different places, which may lead to reproductive isolation if these genes turn out to be incompatible with each other. There is a particular difficulty if adaptation depends on gene combinations that cannot increase from low frequency and that therefore tend to be contained behind narrow "tension zones" (KEY 1968). The spread of such gene combinations requires a "shifting balance" between different evolutionary forces (WRIGHT 1932).

Here we consider the effect of a local barrier to gene flow on the spread of a favorable allele through a continuous habitat. We consider the two qualitatively different cases, first, where the favorable allele can increase from low frequency, and second, where it must increase above some threshold before it can be established by selection. We begin by setting out exact calculations for infinite populations, and then use simulations to show how random genetic drift can increase the delay caused by a barrier. These results are relevant to the key question of how far adaptation and divergence are affected by population subdivision.

Gene flow may be impeded by a physical barrier, caused by a reduction in density or dispersal, or by a genetic barrier, caused by incompatibilities at other loci that cause a reduction in the fitness of hybrid populations. Provided that selection on the locus in question is weak, both physical and genetic barriers can be seen as causing a sharp change in gene frequency, Δp, whose size is proportional to the gradient in frequency on either side, $\partial p/\partial x$; the strength of the barrier is given by a single quantity with the dimensions of a distance: $B = \Delta p/(\partial p/\partial x)$ (NAGYLAKI 1976; BARTON 1979a 1986). We use this approximation throughout, and thus do not consider the detailed effects of barriers that are not localized, and that may be due to selection on many loci. We only consider short-range dispersal; our simulations involve exchange between nearest neighbours, and our analytic results approximate gene flow by diffusion. Thus, we avoid the complexities of long-range dispersal (see MOLLISON 1977; SHAW 1995). The final restriction is that we deal with the spread of an allele at a single locus; this choice is made partly for simplicity, but also because our study is motivated by observations on the distribution of underdominant chromosomal rearrangements.

In the next section, we review analytic results based on the diffusion approximation, and use deterministic calculations for a one-dimensional habitat to test their accuracy. Since the effects of spatial subdivision are likely to be most important in sparse populations, we

Corresponding author: Nick H. Barton, Institute of Cell, Animal, and Population Biology, University of Edinburgh, Edinburgh EH9 3JT, United Kingdom. E-mail: n.barton@ed.ac.uk

then use stochastic simulations in one and two dimensions to find how random drift affects the spread of favorable alleles. In the DISCUSSION, we consider the implications of our results for the movement of tension zones, and in particular, for the spread of chromosome rearrangements.

THE DETERMINISTIC CASE

Diffusion through a continuous habitat: Provided that allele frequencies change slowly in space and time, and provided that long-range dispersal is sufficiently rare, the effects of gene flow can be approximated as a diffusion through a continuous habitat (NAGYLAKI 1975). With discrete generations, the rate of diffusion is given by σ^2, the variance of the distance moved by an individual from its birthplace to a new place of breeding along a particular axis. (With overlapping generations, σ^2 is the variance of distance moved per unit time). In one-dimensional stepping stone models, we define the migration rate m as the probability that an individual will move to either of the two adjacent demes. In two dimensions, we define m as the chance that an individual moves to any of the four adjacent demes. [This definition was used by SLATKIN and BARTON (1989); in two dimensions, it differs by a factor of two from that used in BARTON and ROUHANI (1991) and other papers]. If the deme spacing is ϵ, then the relationship between the two parameters is $\sigma^2 = m\epsilon^2$ in one dimension, and $\sigma^2 = m\epsilon^2/2$ in two dimensions.

Under the diffusion approximation, a barrier that is restricted to a narrow region causes a sharp step in gene frequency Δp. The gradients in gene frequency on either side ($(\partial p/\partial x)_-$, $(\partial p/\partial x)_+$) are proportional to the flux of genes flowing in either direction ($J_+ = (\sigma^2/2)(\partial p/\partial x)_+$; NAGYLAKI 1976; BARTON 1986) and are also proportional to the size of the step. The ratio between step size and the gradient in allele frequency ($B_+ = \Delta p/(\partial p/\partial x)_+$) gives a measure of the barrier to gene flow in either direction. This has the dimensions of a distance. If the barrier is asymmetrical ($B_+ \neq B_-$), then the gradients of allele frequency will differ on the two sides. In a stepping stone model, a local barrier corresponds to a reduction in the migration rate between adjacent demes by a factor k [*i.e.*, from $m/2$ to $m/(2k)$ in one dimension, or from $m/4$ to $m/(4k)$ in two]. This causes an increase in the gradient of allele frequency by a factor k, and hence produces an extra step in allele frequency of $\Delta p = (k-1)\epsilon(\partial p/\partial x)$, where ϵ is the deme spacing. Hence, the barrier strength is $B = (k-1)\epsilon$.

Spread of a neutral allele: If two populations that are fixed for different alleles meet in a sharp step, the discontinuity between them will be smoothed out by gene flow. The decay of this initial step with time can be approximated by a diffusion equation:

$$\frac{\partial p}{\partial t} = \frac{\sigma^2}{2}\frac{\partial^2 p}{\partial x^2}, \tag{1}$$

where x is distance, and covers an infinite range (FISHER 1937; HALDANE 1948). This equation has a solution given by the integral of the normal distribution, with variance $\sigma^2 t$. The collapse of the gradient can be measured by the cline width w, which is defined as the inverse of the maximum slope of the gene frequency cline $p(x)$ (MAY *et al.* 1975). In this case, $w = \sqrt{2\pi\sigma^2 t}$. Equation 1 can also be solved explicitly if the mixing of populations is impeded by a barrier. The solution is a sum of Gaussian integrals; it shows that the delay caused by the barrier is proportional to $(B/\sigma)^2$ (BARTON 1979a).

Spread of an advantageous allele: Suppose now that one allele has an advantage S over the other and there is no dominance; the diffusion approximation requires that S be small. Equation 1 now includes an extra term representing selection:

$$\frac{\partial p}{\partial t} = \frac{\sigma^2}{2}\frac{\partial^2 p}{\partial x^2} + Spq. \tag{2}$$

FISHER (1937) showed that Equation 2 has a family of solutions, each consisting of a wave with constant shape, which advances at a characteristic speed. He argued that the relevant solution was that with the minimum speed, $c = \sigma\sqrt{2S}$. Subsequent numerical and analytic work has confirmed that though solutions exist in which a broad wave advances rapidly, random fluctuations at the leading edge, or boundary effects, tend to slow this down to Fisher's solution. (This kind of wave is referred to as a "pulled" wave, since its speed is determined by the leading edge; STOKES 1976). The diffusion approximation (Equation 2) is only valid if long-distance dispersal is sufficiently rare: the dispersal distribution must fall away at least exponentially (MOLLISON 1977). Otherwise, long-range migrants can establish new centres of increase, so that advance is by sporadic outbreak rather than by a smooth wave (MOLLISON 1977; SHAW 1995).

Since Fisher's solution to Equation 2 has not been derived analytically, it is unlikely that the effect of a barrier can be found explicitly. On dimensional grounds, the delay T should depend on the dimensionless parameter $\tilde{B} = (B/\sigma)\sqrt{2S}$, having the form $ST = f(\tilde{B})$. BARTON (1979a) gave the approximation $ST = \log(\sqrt{\pi}\tilde{B}/2)$ for a very strong barrier. This is the time taken to increase to $p = 0.5$ from a threshold frequency u_0. This threshold is chosen to be the time at which the allele begins to increase faster by selection than by the flux across the barrier. The argument ignores the effect of diffusion. A slightly more accurate argument, which takes into account diffusion and avoids using an arbitrary threshold frequency, is given in APPENDIX A. This also scales with $\log(\tilde{B})/S$: the crucial point is that

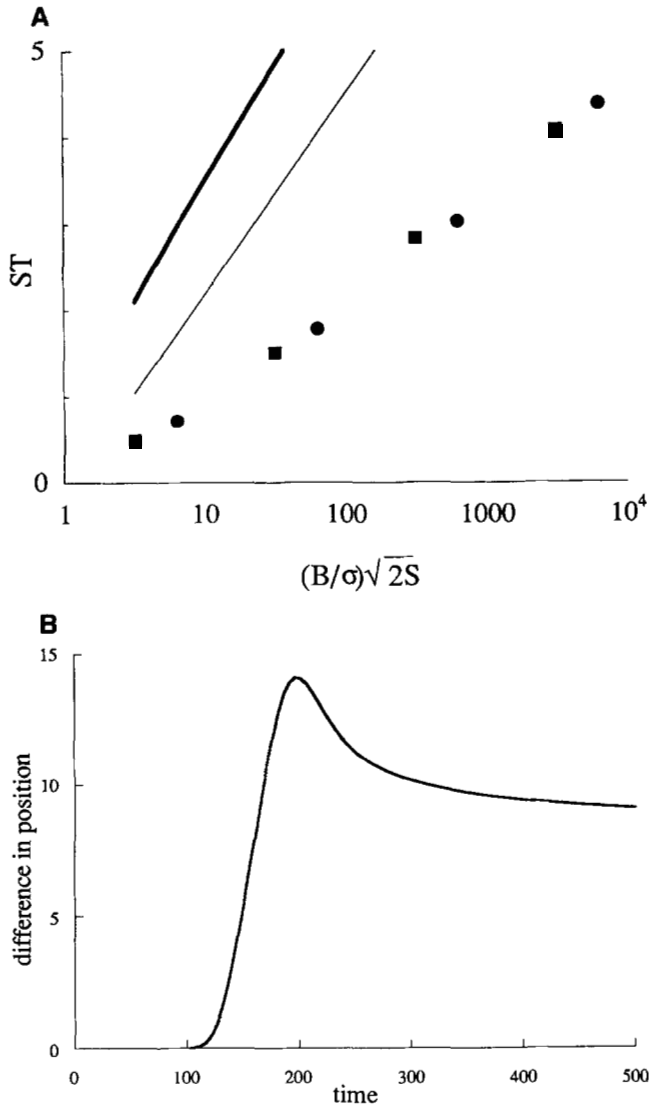

FIGURE 1.—(A) The delay to the advance of an advantageous allele, T, plotted as a function of barrier strength. Results are scaled so that if the diffusion approximation of Equation 2 is valid, the same relation should be obtained for all σ, S: thus, ST is plotted against $\log(\tilde{B})$, where $\tilde{B} = (B/\sigma)\sqrt{2S}$. The heavy line gives the approximation derived from Equation 4, and the light line the approximation $ST = \log(\sqrt{\pi}\tilde{B}/2)$ of BARTON (1979a). Circles give results from a one-dimensional stepping-stone model with $m = 0.5$ and $S = 0.1$; squares give results for $S = 0.025$. One hundred forty demes were used, with a barrier to the right of deme 40; initially, the 10 leftmost demes were fixed. The delay was calculated from the difference in total number of alleles between the solutions with and without a barrier, after the wave had passed the barrier. (B) The difference in position between the waves with and without the barrier. Note that the delay decreases from a maximum after the wave passes the barrier. This is because the wave is broadened by the barrier and hence moves faster.

the delay only increases logarithmically with barrier strength, and hence is small even for a very strong barrier.

Figure 1A compares these approximations with deterministic calculations for $S = 0.025$ and $S = 0.1$. Results for these two selection pressures fall on the same line (compare circles and squares), showing that the diffusion scaling is accurate. The delay does indeed increase logarithmically with barrier strength, but is much less than predicted by either approximation: the best fit for $S = 0.1$ is $ST = 0.53 \log(0.53(B/\sigma)\sqrt{(2S)})$, and $0.52 \log(0.71(B/\sigma)\sqrt{2S})$ for $S = 0.025$. The delay is less than expected because when the barrier is strong, the allele has time to spread over a large distance before it increases to appreciable frequency. Hence, the initial wave of advance is broad, and so advances more quickly, reducing the delay; it settles to a solution to Equation 2, but one with higher speed than the minimum. Over time, it converges on the solution to Equation 2 that has minimum speed, $\sigma\sqrt{2S}$ (STOKES 1976). This can be seen in Figure 1B, which shows the difference in total allele frequency between a freely advancing wave, and a wave that is impeded by a barrier of strength $B = 1000$. The difference in positions increases to a maximum as the wave meets the barrier, but then decreases, because the wave moves faster for some time after it escapes from the barrier. Because the rate at which this "pulled" wave slows down depends on random fluctuations at the leading edge, the delay may be sensitive to details of the model such as deme spacing and dispersal distribution.

Selection against heterozygotes: If heterozygotes are less fit than the average of the two homozygotes (*i.e.*, if there is "underdominance," with fitnesses $1{:}1 + S - s{:}1 + 2S$), then the allele will spread more slowly than the rate $\sigma\sqrt{2S}$ predicted by Equation 2. There are two alternative predictions for the wave speed. First, when the allele can increase from low frequency ($S > s$), consideration of the leading edge ($p \ll 1$) shows that there is a family of solutions, with minimum speed $c = \sigma\sqrt{2(S - s)}$; these are pulled waves (HADELER 1976). Second, there is always a solution that follows a logistic (or tanh) curve, with $p = 1/(1 + \exp(-4(x - ct)/w))$, and width $w = \sigma\sqrt{8/s}$; this has speed $c = S\sigma/\sqrt{2s}$; a perturbation analysis shows that this is the solution for $S \ll s$ (BARTON 1979b). This solution is referred to as a "pushed" wave, since its speed depends on the way selection acts over the whole cline. Numerical results from stepping stone models show that the wave speed is given by $S\sigma/\sqrt{2s}$ for $S < 2s$, and by $\sigma\sqrt{2(S - s)}$ when $S > 2s$ (Figure 2). These results also show that the diffusion approximation is accurate for fairly strong selection ($S = 0.1$).

If heterozygotes are fitter than the original homozygote ($S > s$), then the invading allele can increase exponentially from an indefinitely low frequency. The delay therefore increases logarithmically with barrier strength, as in the case of additive selection (Figure 1A). The effect of a barrier is qualitatively different if the allele cannot increase from low frequency (*i.e.*, if $S < s$). In

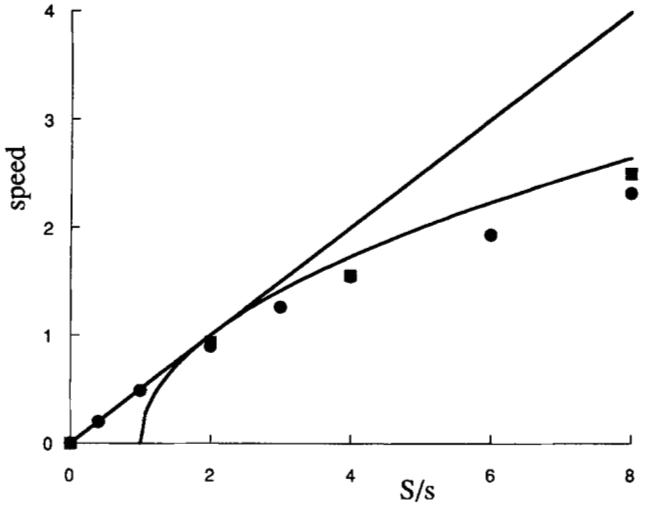

FIGURE 2.—The speed of a wave of advance, as a function of the degree of underdominance (S/s). The upper straight line shows the speed of the tanh solution, $c = S\sigma/\sqrt{2s}$, while the lower curve shows FISHER's (1935) minimum speed, predicted by considering the leading edge, $\sigma\sqrt{2(S - s)}$. The speed c is scaled relative to $\sigma\sqrt{2s}$. Circles are for $s = 0.025$, and squares are for $s = 0.005$. These results are from a stepping-stone model with $m = 0.5$, starting with the leftmost 10 demes fixed, as for Figure 1. The speed was estimated by regressing total allele frequency Σp against time.

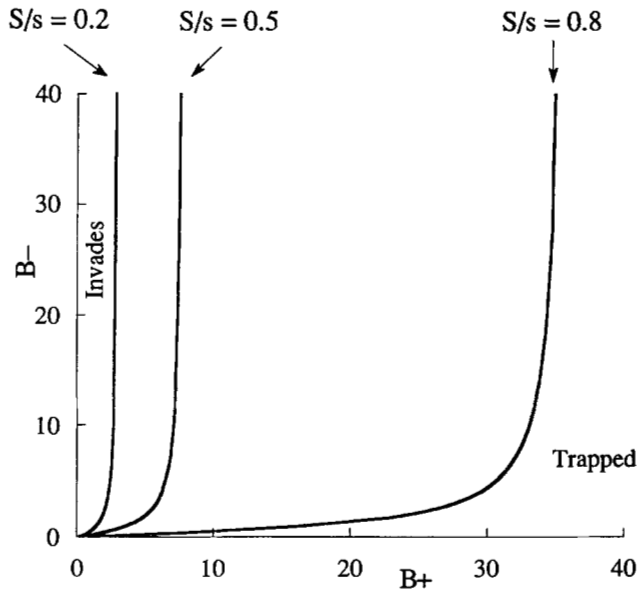

FIGURE 3.—These graphs show the critical combinations of barrier strengths that prevent an allele from invading; barrier strengths are scaled relative to the distance $\sigma/\sqrt{2s}$. From left to right, the curves are for $S/s = 0.2$, 0.5, 0.8. The allele is spreading from right to left; the horizontal axis shows the critical B_+, while the vertical axis shows the critical B_-. The allele will be trapped if the barrier to flow to the right is too strong (B_+ right of the curve) or if the barrier to flow to the left is too weak (B_- below the curve). If the barrier to flow to the right is too strong, the allele cannot advance, even if there is free flow in the opposite direction ($B_- = 0$; threshold B_+ is 2.92, 7.69, 35.69 for $S/s = 0.2$, 0.5, 0.8, respectively).

this case, a sufficiently strong barrier can prevent spread altogether: an equilibrium will be reached in which the flux across the barrier is balanced by selection against the invading alleles. We first find this equilibrium, and hence the critical barrier strength needed to prevent invasion, and then give numerical results for the delay caused when the barrier is below the critical value.

Including selection against heterozygotes in Equation 2 gives

$$\frac{\partial p}{\partial t} = \frac{\sigma^2}{2}\frac{\partial^2 p}{\partial x^2} + Spq - s(p - q)$$

$$= \frac{\sigma^2}{2}\frac{\partial^2 p}{\partial x^2} + 2spq(p - p_0), \quad (3)$$

where $p_0 = (s - S)/2s$ is the threshold frequency below which the allele is selected against; as before, the range of x is from $-\infty$ to ∞. At equilibrium, Equation 3 can be integrated

$$\frac{\partial p}{\partial x} = \frac{1}{\sigma}\sqrt{\frac{2s}{3}}\sqrt{C + p^2(6p_0 - 4p(1 + p_0) + 3p^2)}. \quad (4)$$

Applying the boundary conditions that p tends to 1 on the left, and 0 on the right, determines the constant of integration, C, on either side of the barrier. At the barrier (taken to be at $x = 0$), the gradient is equal to the ratio between the step in allele frequency and the barrier strength. This gives two simultaneous equations for the allele frequencies on either side of the barrier, p_-, p_+,

$$\left(\frac{\partial p}{\partial x}\right)_- = -\frac{(p_- - p_+)}{B_-}$$

$$= \frac{q_-}{\sigma}\sqrt{\frac{2s}{3}(6q_0 - 4q_-(1 + q_0) + 3q_-^2)}, \quad (5a)$$

$$\left(\frac{\partial p}{\partial x}\right)_+ = -\frac{(p_- - p_+)}{B_+}$$

$$= \frac{p_+}{\sigma}\sqrt{\frac{2s}{3}(6p_0 - 4p_+(1 + p_0) + 3p_+^2)}. \quad (5b)$$

These equations can be solved numerically for given barrier strengths (B_-, B_+) and threshold frequency (p_0). To find the critical barrier strengths which prevent invasion, rewrite Equation 5a as an expression for B_-, as a function of q_-. This has a minimum, which gives the critical B_- for given p_+. Equation 5b then gives the value of B_+ as a function of p_+ at the critical point.

Figure 3 shows the critical combinations of barrier strengths; the three curves correspond to $S/s = 0.2$, 0.5, 0.8. If B_+ is sufficiently strong (right of Figure 3), or if B_- is sufficiently weak (below curves on Figure 3), then the allele cannot invade. Figure 4 shows the delay as a function of barrier strength, calculated from a stepping-stone model. This increases to infinity at the critical

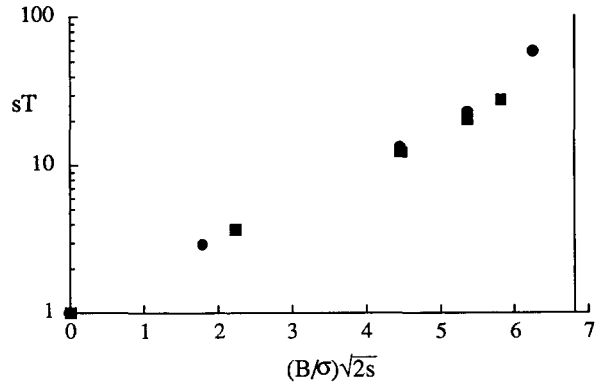

FIGURE 4.—The delay to the spread of an allele as a function of barrier strength, for a one-dimensional stepping stone model with $m = 0.5$. Squares show results for $S = 0.025$, $s = 0.05$ giving fitnesses 1:0.975:1.05; circles show results for $S = 0.1$, $s = 0.2$ giving fitnesses 1:0.9:1.2. Results are scaled relative to the time $1/s$ and distance $\sigma/\sqrt{2s}$; the graph should thus be independent of selection strength. The critical barrier strength is at $B_+ = B_- = 6.82\sigma/\sqrt{2s}$ (see Figure 3).

barrier strength and can be large below this value. (Note that the delay is plotted as sT, on a log scale). The effect of a barrier is much greater than for an allele that is favored in the heterozygote, because the allele must build up above a threshold frequency before its spread is assisted by selection.

THE EFFECTS OF RANDOM DRIFT

We now consider the effects of random drift on the spread of an advantageous allele, treating the models in the same order as in the previous section. The stochastic problem is harder to treat, because simulations are slower and must be replicated. Moreover, the effects of random drift are qualitatively different in one and two dimensions (MALÉCOT 1948), and so both cases must be treated.

The stochastic simulation: The effect of barriers, deme size and selection on the time needed for fixation of a favored allele was studied using a stepping-stone model. Throughout, we use the convention that the deme spacing is $\epsilon = 1$, so that the deme size is $N = \rho$. Initially, different alleles were fixed on either side of a barrier at $x = 0$, representing secondary contact between diverged populations. There was no migration beyond the bounds of the array. The time delay, T, due to a barrier was estimated by subtracting the mean time to fixation without a barrier from that with a barrier.

In one dimension, simulations were run using Mathematica (WOLFRAM 1991). Selection acted on a large number of diploid juveniles; the recursion for change in allele frequency is $p' = p(1 + 2S - qs))/(1 + 2pS - 2pqs)$. A fraction m of these then migrated, half to the left and half to the right. N diploid parents were then sampled; the next generation was formed by random union of a large number of gametes. The number of demes and position of the barrier were chosen to avoid edge effects; most runs used 41 demes, with a barrier between demes 6 and 7.

To increase speed, simulations in two dimensions were run using a program written in Pascal; 20×10 demes were simulated, with the allele advancing along the axis of length 20 demes. Runs were terminated at 10,000 generations, or when the advantageous allele was completely fixed; the time at which the latter occurred was taken to be the time to fixation. The two-dimensional simulation differed slightly, in that migration is by a small number of adults, rather than by a large number of juveniles. Random fluctuations therefore occur both through the random sampling of migrants between demes and through random variation in reproductive success within demes. Such stochastic migration can alter spatial correlations, and increases the variance of gene frequency above that expected due to sampling drift alone (see EPPERSON 1994). For example, in systems where the stochastic variance occurs from random sampling of a migrant group of size $2Nm$, the variance of gene frequencies can be increased up to double that for the corresponding case of deterministic migration; this is because there are two rounds of sampling rather than one (EPPERSON 1994).

In each generation, the number of migrants from a deme was taken from the binomial distribution with parameters m, N, where m is migration rate and N is the number of adult individuals in the deme before migration. Genotypes of migrants were assigned randomly from the genotypes within the deme of origin after random drift. Sampling was without replacement. Parents were expected to produce an infinite number of gametes and therefore selection on gametes was a deterministic process, as in the one-dimensional simulations.

All procedures used to simulate migration, random drift and selection were checked against theoretical expectations. The probability and rate of fixation of a neutral allele without migration agreed with a Markovian transition probability matrix for a single deme; the fixation probability of an advantageous allele (with and without migration) was $2S$ for small S. Stochastic migration was checked against the decay of cline width of a neutral allele (from Equation 1) and also agreed closely with theory.

Spread of an advantageous allele: Mathematical analysis of the interaction between selection, gene flow and drift is in general intractable. However, we can use some heuristic arguments to illuminate the simulation results. First, consider the spread of an advantageous allele in the absence of a barrier. Taking expectations of Equation 2,

$$\frac{\partial \overline{p}}{\partial t} = \frac{\sigma^2}{2}\frac{\partial^2 \overline{p}}{\partial x^2} + S(\overline{pq} - \mathrm{var}(p))$$

$$= \frac{\sigma^2}{2}\frac{\partial^2 \overline{p}}{\partial x^2} + S\overline{pq}(1 - F). \quad (6)$$

Since the variance in allele frequency produced by random drift reduces the proportion of heterozygotes by a fraction F, it will reduce the response to selection and slow the advance of the wave; the effective selection coefficient is reduced to $S(1 - F)$. In a spatially uniform polymorphism with stability S and population density $\rho = N/\epsilon^2$, the standardized variance $F = \mathrm{var}(p)/\overline{pq}$ would be constant, and equal to $1/(1 + 4\rho\sigma\sqrt{2S})$ in one dimension, and $1/(1 + 4\pi\rho\sigma^2/\ln(1/\sqrt{2S}))$ in two dimensions (MALÉCOT 1948). NAGYLAKI (1978) showed that in a one-dimensional cline, F depends on the dimensionless quantity $\rho\sigma\sqrt{2S}$, being inversely proportional to it for large values, and tending to 1 for small values. If we assume F has the same form for a wave of advance, then we expect a speed

$$c = \frac{c_0}{\sqrt{1 + \dfrac{A}{\rho\sigma\sqrt{2S}}}} \quad \text{(one dimension)}, \qquad (7a)$$

$$c = \frac{c_0}{\sqrt{1 + \dfrac{A}{(4\pi\rho\sigma^2)}}} \quad \text{(two dimensions)}, \qquad (7b)$$

where $c_0 = \sigma\sqrt{2S}$ is the deterministic speed corrected for high value of selective advantage used in simulations ($S = 0.1$). Figure 5 compares simulated values of the wave speed with these predictions; A is calculated by least-squares regression of $1/c^2$ on $1/\rho$. There is a good fit, with A estimated as 3.87 in one dimension, and 12.96 in two. This is much greater than the value $A = {}^1/_4$ describing the effect of drift on a uniform polymorphism in one dimension, or $A = \ln(1/\sqrt{2S}) = 0.80$ in two. It seems that random drift reduces heterozygosity in the advancing wave, and hence its rate of advance, much more than would be expected from its effect on neutral polymorphisms.

In the alternative limit of very low density, most demes are likely to be fixed for one or other allele. The probability of fixation of a favorable allele that enters a deme fixed for its homologue is $2S/(1 - \exp(-4NS))$; the converse probability is $2S/(\exp(4NS) - 1)$. There are, on average, Nm such migrants in each direction, and so the expected rate of advance of the boundary between demes fixed for the different alleles is $(Nm)(2S/(1 - \exp(-4NS)) - 2S/(\exp(4NS) - 1)) = 2NmS$ (see SLATKIN and CHARLESWORTH 1978). This approximation is shown by the steep line on the left of Figure 5A.

As well as slowing the advance of the favored allele, drift introduces random variation in its position. Although the mean location of a set of clines will increase linearly with time, at the rate shown in Figure 5, the position of any one cline will vary around this expected position. In each generation, drift introduces a random perturbation that advances or retards the cline by some amount. Since successive perturbations are independent, the variance in position around the expected location increases linearly with time (Figure 6). The variance in position increases at a rate $1.19\sigma/\rho\sqrt{2S}$ (APPENDIX B). This prediction agrees with one-dimensional simulations for high densities ($\rho > 10$), but overestimates the increase in variance for low density (Figure 7). This may be because at low density, drift substantially reduces heterozygosity, and hence wave speed (Figure 5a). In two dimensions, fluctuations at different positions along the wave tend to cancel, so that the variance in overall position should increase with $\sqrt{t}$, rather than linearly with time (BARTON 1979b). However, we were unable to simulate large enough areas to confirm this argument.

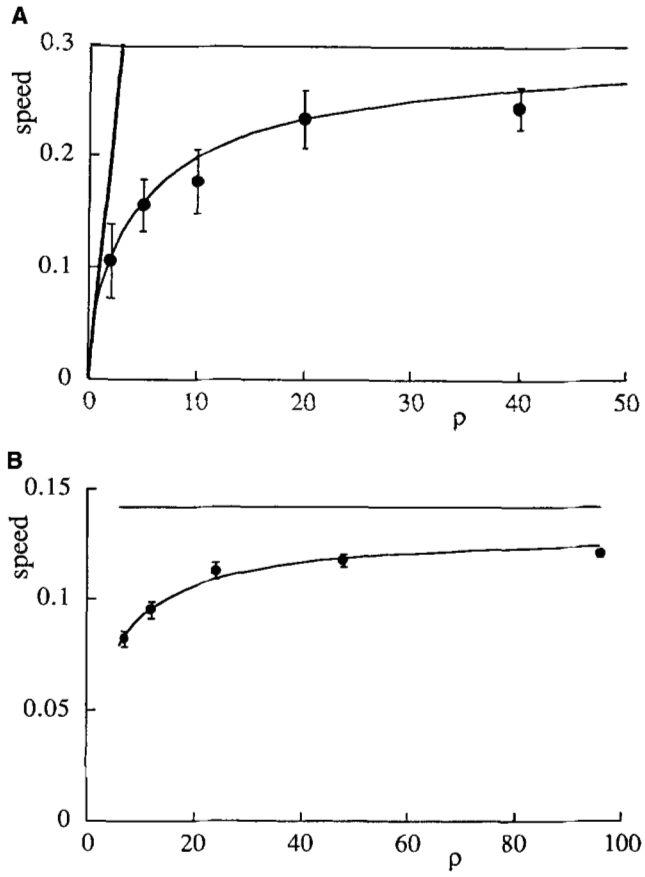

FIGURE 5.—(A) The speed of a wave of advance in one dimension, plotted against deme size. ● show mean speeds from 10 replicates of the stochastic simulation, with 95% confidence limits. ($S = 0.1$, $m = 0.5$; 60 demes, starting with the leftmost six fixed). The curve shows the predicted relationship from Equation 9, with $A = 3.87$ calculated by least-squares regression of $1/c^2$ against $1/\rho$. The horizontal line shows the deterministic speed, $\sigma\sqrt{2S}$, while the steep line to the left shows the approximation for small ρ, $c = 2\rho\sigma^2 S$. (B) The corresponding graph, for two dimensions. ($S = 0.1$, $m = 0.2$; 60×10 demes, starting with the leftmost 6×10 fixed; $A = 12.96$).

Spread of an advantageous allele past a barrier: In the deterministic case, we showed that even a strong barrier has little effect on an advantageous allele: be-

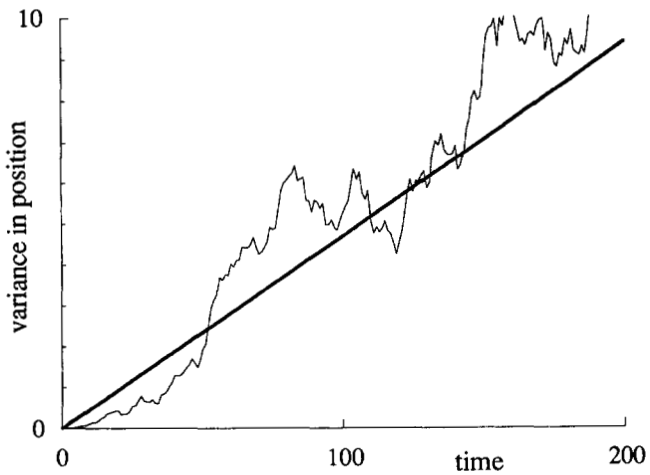

FIGURE 6.—The variance around the expected position, plotted against time. The expectation from Equation B1, $1.19/\rho\sigma\sqrt{2S}$ is shown by the straight line. Based on 10 replicates of the stochastic simulation in one dimension. (ρ = 40; S = 0.1, m = 0.5; 60 demes, starting with the leftmost six fixed).

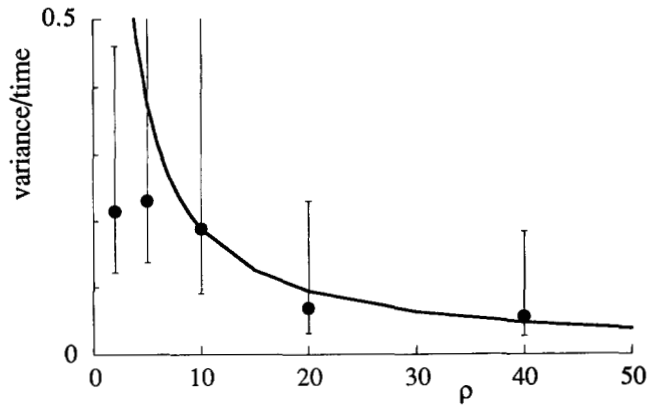

FIGURE 7.—The rate of increase in variance around the expected position in a one-dimensional habitat, plotted against density, ρ. The curve shows the expectation from Equation 10, $1.19/\rho\sigma\sqrt{2S}$. Circles show mean speeds from 10 replicates of the stochastic simulation, with 95% confidence limits. Parameters are as in Figure 6.

cause such an allele can increase exponentially from low frequency, the delay only increases logarithmically with barrier strength. SLATKIN (1976) considered the stochastic case and demonstrated a relation between the delay in time to fixation with decreasing migration rate and the number of individuals within a population. His argument was based on the approximate time to fixation of an advantageous allele within a single population, $(1/S)\ln[2Np(0)]$, where $p(0)$ is the initial allele frequency. However, SLATKIN's formula applies to flow into a single deme, rather than the rate of spread across an array of demes. Here, we combine a heuristic argument with simulation results to show that random drift can substantially enhance the effect of a strong barrier, above that expected in a dense population.

When the barrier is very strong, migrants cross it only rarely. The flux across is $J = (\sigma^2/2)/B$, the density of genes is 2ρ, and so the expected number of genes crossing per generation is $(\rho\sigma^2/B)$. Each of these genes has probability $2S$ of fixing, and so the expected time before an allele begins to fix is $B/(2S\rho\sigma^2)$; we assume $B \gg 2S\rho\sigma^2$, so that only one allele fixes. [Note that the probability of fixation is $2S$, regardless of the presence of the barrier (assumed impermeable) on one side (MARUYAMA 1972)]. There is then a further delay before the allele rises to high frequency and begins to spread as a steady wave. This second delay can readily be calculated. When the allele is rare, its expected frequency (including cases of loss and fixation) is given by Equation 2, and depends on the initial total allele frequency, $1/2\rho$. After a time long enough for the fate of the allele to be decided, but short enough that it is still rare, its expected frequency *given that it will be fixed* is equal to the overall expectation, divided by the probability of fixation, $2S$. Hence, the eventual expected frequency, conditional on fixation, is given by following Equation 2, with initial inoculum $1/4\rho S$; this converges to a wave of advance, with some delay. Scaling arguments show that this delay is, on average, a function $f[\rho\sigma\sqrt{2S}]/S$, where the dimensionless quantity $\rho\sigma\sqrt{2S}$ is a measure of the relative strengths of drift and selection (see NAGYLAKI 1978). Deterministic simulations for $S = 0.1$, $m = 0.5$ show that $f[x] \approx 3.50 + 0.55\ln(x) + 0.0146\ln(x)^2$ (estimated by least squares fit of the delay to $\ln(\rho)$). Overall, therefore, the expected delay is $B/(2S\rho\sigma^2) + f[\rho\sigma\sqrt{2S}]/S$. This increases linearly with barrier strength, rather than logarithmically, showing that drift can substantially amplify the effect of a barrier.

This prediction is compared with simulation results in Figure 8. The lower curve in Figure 8A shows the delay in an infinite population (from Figure 1). This only increases logarithmically with barrier strength, and so is much less than in finite populations. The simulations show that the delay increases linearly with barrier strength, and is greater when density is low (circles: ρ = 20, squares: ρ = 10). There is reasonable agreement with the prediction described above, which is shown by the straight lines for each of the two densities. However, the delay is somewhat lower than predicted for one dimension. The two-dimensional simulations were necessarily run with a short barrier, and so the above argument should apply, with ρ replaced by ρL, where L is the length of the barrier. If the barrier were very long, alleles would cross and begin to fix at many places simultaneously. One should then take into account the time taken for alleles advancing from different points to spread along the barrier from their separate origins; this might increase the delay above the one-dimensional prediction, as is seen in Figure 8B. The relationship between the time delay and the length of the barrier, L, is given in Figure 8C. The graph shows a situation with a strong barrier (B = 500). Here, the

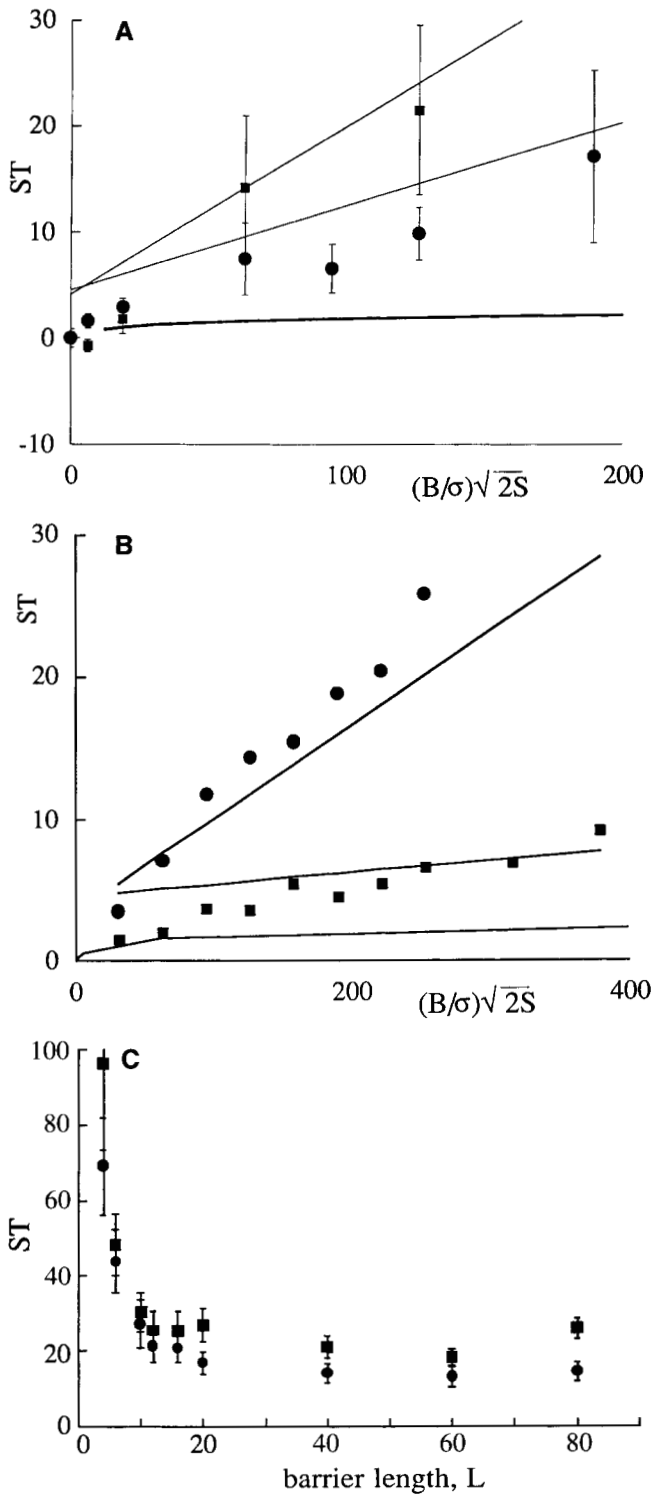

FIGURE 8.—(A) The average delay, T, caused by a barrier in one dimension, plotted against barrier strength. Results are scaled to the dimensionless quantities ST and $\tilde{B} = B\sqrt{2S}/\sigma$. Simulations were run for $S = 0.1$, at a density $\rho = 20$ (●) and $\rho = 10$ (■). Confidence intervals (95%) are shown, derived from 20 replicates. The straight lines show the theoretical predictions for a strong barrier, $B/(2S\rho\sigma^2) + f[\rho\sigma\sqrt{2S}]/S$, for $\rho = 10$ and 20. The deterministic results ($\rho = \infty$) are shown by the lower heavy curve, which is interpolated from the results in Figure 1 for $S = 0.025$. (B) The corresponding graph for two dimensions. Density here was $\rho = 12$ (●, 50 replicates) and $\rho = 96$ (■, 25 replicates), $m = 0.2$, $S = 0.02$. (C) The relationship between the delay caused by the local barrier ($B = 500$) and the length of a barrier L. Squares indicate a scaled delay, ST, for $S = 0.02$, while circles for $S = 0.08$ coming from 100 replicates for $L \leq 20$ and 50 replicates otherwise. $m = 0.2$, $\rho = 12$.

delay is primarily a function of probability that a migrant will cross the barrier. It can be seen the delay decreases inversely with ρL, as argued above.

Escape of a tension zone from a barrier: Suppose now that selection acts against heterozygotes, such that the invading allele cannot increase from low frequency. In the deterministic case, a sufficiently strong barrier will prevent the invasion altogether; instead, the incoming allele will reach an equilibrium between migration across the barrier and selection against it, given by Eq. 5. With finite population size, there is some chance that the allele will drift to high enough frequency to escape the barrier. While it would be hard to calculate the rate of escape, we expect it to decrease exponentially with deme size (see BARTON and ROUHANI 1987, 1991).

Figure 9 shows the average delay as a function of barrier strength. For $(S/s) = 0.5$, the critical barrier strength is $(B/\sigma)\sqrt{2s} = 6.82$, above which the delay becomes infinite in an infinite population (heavy curve in Figure 9). All the simulations were for barriers stronger than this critical value. Random drift can free the favorable allele and so in (almost) all cases the delay decreases as deme size becomes smaller. A similar pattern is seen in two dimensions; there, the delay is closer to the deterministic expectation for $\rho = 96$, and considerably reduced for $\rho = 12$ (Figure 9b). Figure 10A shows the same data, plotted against deme size instead of barrier strength. As expected, the delay increases exponentially with deme size when the barrier is strong (as shown by the approximately linear increase on this log scale for $B = 20$, 30, 40). However, there is little increase in the delay with deme size when the barrier is only just stronger than the critical value [$B = 10$ (circles) *vs.* the critical value of $B = 6.82\sigma/\sqrt{2s} = 7.62$]. Figure 10B shows corresponding results for two dimensions; again, these roughly linear graphs suggest that the delay increases exponentially with deme size. Here, however, the lines for different barrier strengths are more nearly parallel than in one dimension, indicating that an increase in barrier strength increases the delay by the same factor, independent of deme size.

DISCUSSION

The effect of population structure on adaptation depends very much on whether alleles tend to increase even when rare, or must instead rise above some threshold frequency before being favored. These two cases reflect the contrast between Fisher's view of evolution, in which adaptation is most efficient in large populations, with Wright's, in which random drift and re-

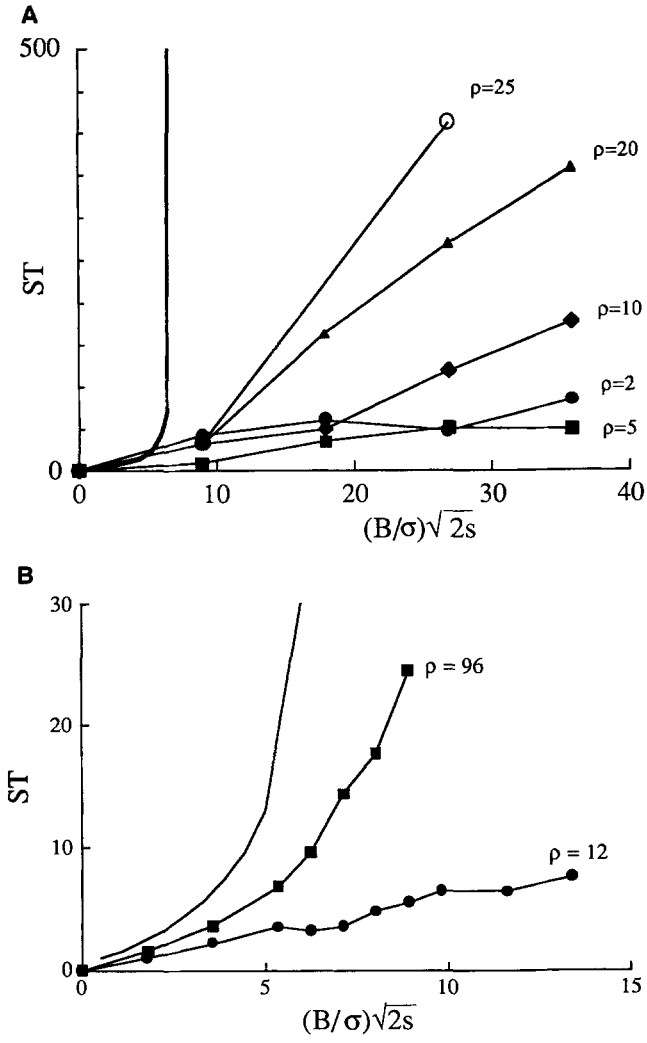

FIGURE 9.—(A) The average delay as a function of barrier strength with heterozygote disadvantage $s = 0.2$, and selective advantages $S = 0.1$, in one dimension; $m = 0.5$. For these parameters, the critical barrier strength is $B_+ = B_- = 6.82\sigma/\sqrt{2s}$ (see Figure 3). Above this value, the delay becomes infinite in an infinite population. Values are based on 20 replicates, for densities $\rho = 2, 5, 10, 20, 25$. (B) Results for two dimensions, using an array of 20 × 10 demes. ($s = 0.04$, $S = 0.02$, $m = 0.2$; for these parameters, the critical barrier strength is $B_+ = B_- = 6.82\sigma/\sqrt{2s}$, as before). Values are based on 50 and 25 replicates, for densities $\rho = 12$ and 96, respectively.

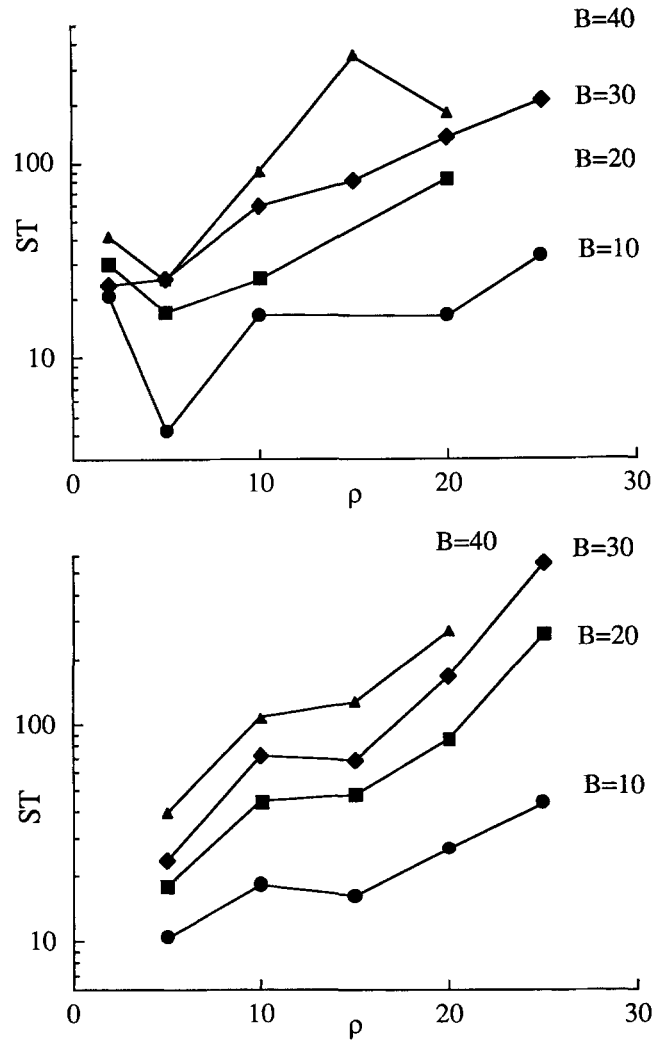

FIGURE 10.—The delay, plotted on a log scale against deme size, for $B = 10, 20, 30, 40$; the data are the same as in Figure 9. (A) One dimension. (B) Two dimensions.

stricted gene flow are essential for continued progress. In the first case, the spread of an allele through a continuous habitat is somewhat slowed by random drift (Figure 5). In a dense population, a local barrier causes a slight delay ($\approx \log(B)$), which can be substantially increased when deme size is low ($\approx B$; Figure 8). In contrast, when selection against the heterozygote prevents increase from low frequency, a local barrier to gene flow can prevent an advantageous allele from spreading through a dense population. Drift can then facilitate the spread and can free an allele that would otherwise be trapped indefinitely. Two-dimensional results are qualitatively similar; the delay caused by a barrier decreases substantially as the length of contact between two races increases. Thus, genetic differentiation will be greater where gene flow is confined to a narrow corridor such as a mountain valley or shoreline.

Our results could be used to describe the spread of any beneficial allele. However, our study was motivated originally by the evolution of chromosome rearrangements, and in particular, by the geographic distribution of centromeric (Robertsonian) fusions in mice and shrews (SEARLE 1993). Here, populations are usually fixed for a particular combination of metacentrics over substantial areas. This suggests that new metacentric fusions are either lost or spread rapidly to fixation. Moreover, the large number of metacentrics that have been derived from the ancestral acrocentric karyotype suggests that they increase the fitness of their carriers. This selective advantage could arise due to a novel reshuffling of genes (WILSON *et al.* 1974), meiotic drive (NACHMAN and SEARLE 1995), reduction in recombination between epistatically interacting genes (CHARLES-

WORTH and CHARLESWORTH 1980; for a mechanism of recombination suppression see DAVISSON and AKESON 1993) or competitive superiority (CAPANNA *et al.* 1984; SCRIVEN 1992). No direct estimates of selective advantage are available. However, analysis of overlapping clines in the hybrid zone between the Oxford and Hermitage races of shrews suggested an advantage of metacentrics over acrocentrics of $S = 2.6\%$ (HATFIELD *et al.* 1992). The hybrids originating from crosses between two chromosome races are expected to suffer partial sterility due to problems at meiosis. Two types of hybrids are found. "Simple" heterozygotes are detected, if one parental race is fixed for one or more fusions while the corresponding arms in the other are acrocentric. These hybrids usually suffer only weak selection (VIROUX and BAUCHAU 1992; WALLACE 1994). "Complex" heterozygotes could arise if their parental races share one arm in two different fusions; this could be due to independent fusions of the same chromosome arm, or whole-arm reciprocal translocation. Where one arm is shared in two fusions (monobrachial homology), hybrids are then expected to suffer strong selection because they form chain or ring configurations at meiosis (CAPANNA *et al.* 1976), and hence a substantial decrease of heterozygote fitness (REDI and CAPANNA 1988; SEARLE 1988).

A particularly well-studied example is found in the Upper Valtellina valley in northern Italy, where four Robertsonian races meet with the all-acrocentric race of the house mouse (*Mus domesticus*) (HAUFFE and SEARLE 1993). The distribution is patchy, one race being usually restricted to one or two villages. In samples collected between 1989 and 1991, most individuals were homozygous, yet hybrids were found in almost every village (HAUFFE and SEARLE 1993). Most villages in Upper Valtellina are divided by natural barriers such as streams, gullies or pasture, which may prevent movement of chromosome races. What can one say on the future evolution of this system? If two races occupy different villages, their stability will depend on the strength of both physical and genetic barriers and population density (*i.e.*, on B, s, and ρ). For example, the Poschiavo (POS, $2n = 26$) and Upper Valtellina (UV, $2n = 24$) races are fixed in four neighboring villages (POS in Migiondo, UV in Sontiolo, Tiolo and Lago). What is the chance that the UV race will invade the POS race? Due to monobrachial homology the fitness of the hybrids between the two races is estimated to be reduced by 30–40% due to chromosome nondisjunction at meiosis (HAUFFE 1993). Based on capture-recapture study in the same area, the deme size varies between 1 and 23 mice, and there are ~50 potential breeding sites (demes) in each village with the average distance between demes $\epsilon \approx 33$ m (H. HAUFFE, unpublished data). Tiolo and Sontiolo are isolated by a distance of 500 m from Migiondo, corresponding to 15 interdeme distances. In addition, these villages are separated by a fast-flowing river and a motorway. This should greatly increase the effective interdeme distance; we chose 20 here as a conservative estimate. Hence, physical barriers could decrease migration rate by ~20 times. Taking selection against hybrids as $s = 0.3$ and m as 0.2, it leads to a value of the scaled barrier $(B/\sigma)\sqrt{2s} \approx 48$. The critical values for barriers with $S/s = 0.5$ and 0.8 are 7.69 and 35.69, respectively. Both the theoretical values are below the estimates from the field data, which means that the barrier could be overcome by a combination of drift and a rather high selective advantage to the homozygote ($S > 0.2$). While the field data have supported the presence of random drift, there is no evidence for the high advantage that would be necessary to break these barriers. Therefore we conclude that the distribution of both POS and UV races will be stable until the population is disrupted by some extrinsic catastrophe.

Many other animal species have their range divided into subpopulations differing in chromosome arrangement (WHITE 1978; BARTON and HEWITT 1985; KING 1993). These chromosomal races are often associated with physical barriers such as streams, rivers, roads, gullies or inhospitable areas [see SAGE *et al.* (1993) for a review on mice; MERCER and SEARLE (1991): shrews in Scotland; BRÜNNER *et al.* (1994): shrews in Switzerland; PATTON (1993): pocket gophers in northern America; NEVO and BAR-EL (1976): mole rats in Israel; BARTON and GALE (1993): grasshoppers in the Alps Maritimes]. Such barriers increase the chance that a chromosomal mutation will rise to high frequency despite selection against the heterozygote (LANDE 1979), but as our analysis shows, impedes its subsequent spread. The fate of chromosome races, or more generally, of novel "adaptive peaks," may therefore depend more on the chance factors that influence the distribution of the species, than on the adaptive competition between gene combinations envisaged by WRIGHT (1932) in his theory of the "shifting balance."

We are specially grateful to H. C. HAUFFE for allowing us to present her unpublished data. B. NÜRNBERGER, J. B. SEARLE, H. C. HAUFFE, S. BAIRD, L. KRUUK and two anonymous referees gave constructive comments on the manuscript. The work was supported by the European Union (Human Capital and Mobility Contract No. ERB4050PL922765).

LITERATURE CITED

BARTON, N. H., 1979a Gene flow past a cline. Heredity **43:** 333–339.

BARTON, N. H., 1979b The dynamics of hybrid zones. Heredity **43:** 341–359.

BARTON, N. H., 1986 The effects of linkage and density-dependent regulation on gene flow. Heredity **57:** 415–426.

BARTON, N. H., and K. S. GALE, 1993 Genetic analysis of hybrid zones, pp. 13–45 in *Hybrid Zones and the Evolutionary Process*, edited by R. G. HARRISON. Oxford University Press, Oxford.

BARTON, N. H., and G. M. HEWITT, 1985 Analysis of hybrid zones. Ann. Rev. Ecol. Syst. **16:** 113–148.

BARTON, N. H., and S. ROUHANI, 1987 The frequency of shifts between alternative equilibria. J. Theor. Biol. **125:** 397–418.

BARTON, N. H., and S. ROUHANI, 1991 The probability of fixation of a new karyotype in a continuous population. Evolution **45:** 499–517.

BRÜNNER, H., L. FUMAGALI and J. HAUSSER, 1994 A comparison of two contact zones between chromosomal races of *Sorex araneus* in the Western Alps: karyology and genetics. Folia Zool. **43**(Suppl. 1): 113.

CAPANNA, E., M. CORTI, D. MAINARDI, S. PARMIGIANI and P. F. BRAIN, 1984 Karyotype and intermale aggression in wild house mice: ecology and speciation. Behav. Genet. **14:** 195–208.

CAPANNA, E., A. GROPP, H. WINKING, G. NOACK and M.-V. CIVITELLI, 1976 Robertsonian metacentrics in the mouse. Chromosoma **58:** 341–353.

CHARLESWORTH, D., and B. CHARLESWORTH, 1980 Sex differences in fitness and selection for centric fusions between sex chromosomes and autosomes. Genet. Res. **35:** 205–214.

DAVISSON, M. T., and E. C. AKESON, 1993 Recombination suppression by heterozygous Robertsonian chromosomes in the mouse. Genetics **133:** 649–667.

EPPERSON, B. K., 1994 Spatial and space-time correlations in systems of subpopulations with stochastic migration. Theor. Pop. Biol. **46:** 160–197.

FISHER, R. A., 1937 The wave of advance of advantageous genes. Ann. Eugenics **7:** 355–369.

HADELER, K. P., 1976 Travelling population fronts, pp. 585–592 in *Population Genetics and Ecology*, edited by S. KARLIN and E. NEVO. Academic Press, New York.

HALDANE, J. B. S., 1948 The theory of a cline. J. Genet. **48:** 277–284.

HATFIELD, T., N. BARTON and J. B. SEARLE, 1992 A model of a hybrid zone between two chromosomal races of the common shrew (*Sorex araneus*). Evolution **46:** 1129–1145.

HAUFFE, H. C., 1993 *Robertsonian Fusions and Speciation in a House Mouse Hybrid Zone.* PhD. Thesis, University of Oxford.

HAUFFE, H. C., and J. B. SEARLE, 1993 Extreme karyotypic variation found in a mottled hybrid zone between five chromosomal races of *Mus musculus domesticus* in Upper Valtellina, Northern Italy. The tobacco mouse story revisited. Evolution **47:** 1374–1395.

KEY, K. H. L., 1968 The concept of stasipatric speciation. Syst. Zool. **17:** 14–22.

KING, M., 1993 *Species Evolution: The Role of Chromosome Change.* Cambridge University Press, Cambridge.

LANDE, R., 1979 Effective deme sizes during long-term evolution estimated from rates of chromosomal rearrangement. Evolution **33:** 234–251.

MALÉCOT, G., 1948 *Les Mathématiques de l'Hérédité.* Masson, Paris.

MARUYAMA, T., 1972 On the fixation probability of mutant genes in a subdivided population. Genet. Res. **15:** 221–225.

MAY, R. M., J. A. ENDLER and R. E. MCMURTRIE, 1975 Gene frequency clines in the presence of selection opposed by gene flow. Am. Nat. **109:** 659–676.

MERCER, S., and J. B. SEARLE, 1991 Preliminary analysis of a contact zone between karyotypic races of the common shrew (*Sorex araneus*) in Scotland. Mém. Soc. Vaud. Sci. Nat. **19:** 73–78.

MOLLISON, D., 1977 Spatial contact models for ecological and epidemic spread. J. R. Statist. Soc. B **39:** 283–326.

NACHMAN, M. W., and J. B. SEARLE, 1995 Why is the house mouse karyotype so variable? Trends Ecol. Evol. **10:** 397–402.

NAGYLAKI, T., 1975 Conditions for the existence of clines. Genetics **80:** 595–615.

NAGYLAKI, T., 1976 Clines with variable migration. Genetics **83:** 867–886.

NAGYLAKI, T., 1978 Random genetic drift in a cline. Proc. Natl. Acad. Sci. USA **75:** 423–426.

NEVO, E., and H. BAR-EL, 1976 Hybridization and speciation in fossorial mole rats. Evolution **30:** 831–840.

PATTON, J. L., 1993 Hybridization and hybrid zones in pocket gophers (Rodentia, Geomyidae), pp. 290–308 in *Hybrid Zones and the Evolutionary Process*, edited by R. G. HARRISON. Oxford University Press, Oxford.

REDI, C. A., and E. CAPANNA, 1988 Robertsonian heterozygotes in the house mouse and the fate of their germ cells, pp. 315–359 in *The Cytogenetics of Mammalian Autosomal Rearrangements*, edited by A. DANIEL. Alan R. Liss, New York.

SAGE, R. D., W. R. ATCHLEY and E. CAPANNA, 1993 House mice as models in systematic biology. Syst. Biol. **42:** 523–561.

SCRIVEN, P. N., 1992 Robertsonian translocations introduced into an island population of house mice. J. Zool. **227:** 493–502.

SEARLE, J. B., 1988 Selection and Robertsonian variation in nature: the case of the common shrew, pp. 507–531 in *The Cytogenetics of Mammalian Autosomal Rearrangements*, edited by A. DANIEL. Alan R. Liss, New York.

SEARLE, J. B., 1993 Chromosomal hybrid zones in Eutherian mammals, pp. 309–353 in *Hybrid Zones and the Evolutionary Process*, edited by R. G. HARRISON. Oxford University Press, Oxford.

SHAW, M. W., 1995 Simulation of population expansion and spatial pattern when individual dispersal distributions do not decline exponentially with distance. Proc. R. Soc. London B **259:** 243–248.

SLATKIN, M., 1976 The rate of spread of an advantageous allele in a subdivided population, pp. 767–780 in *Population Genetics and Ecology*, edited by S. KARLIN and E. NEVO. Academic Press, New York.

SLATKIN, M., and N. H. BARTON, 1989 A comparison of three methods for estimating average levels of gene flow. Evolution **43:** 1349–1368.

SLATKIN, M., and D. CHARLESWORTH, 1978 The spatial distribution of transient alleles in a subdivided population: a simulation study. Genetics **89:** 793–810.

STOKES, A. N., 1976 On two types of moving front in quasilinear diffusion. Math. Biosci. **31:** 307–315.

VIROUX, M.-C., and V. BAUCHAU, 1992 Segregation and fertility in *Mus musculus domesticus* (wild mice) heterozygous for the Rb(4.12) translocation. Heredity **68:** 131–134.

WALLACE, B. M. N., 1994 A comparison of meiosis and gametogenesis in homozygotes and simple Robertsonian heterozygotes of the common shrew (*Sorex araneus*) and house mouse (*Mus musculus domesticus*). Folia Zool. **43**(Suppl. 1): 89–96.

WHITE, M. J. D., 1978 *Modes of Speciation.* W. H. Freeman, San Francisco.

WILSON, A. C., V. M. SARICH and L. MAXSON, 1974 The importance of gene rearrangement in evolution: evidence from studies on rates of chromosomal, protein, and anatomical evolution. Proc. Natl. Acad. Sci. USA **71:** 3028–3030.

WOLFRAM, S., 1991 *Mathematica.* Addison Wesley, New York.

WRIGHT, S., 1932 The roles of mutation, inbreeding, crossbreeding and selection in evolution. Proc. 6th Int. Cong. Genet. **1:** 356–366.

Communicating editor: M. SLATKIN

APPENDIX A: SPREAD PAST A STRONG BARRIER

If the barrier is strong, an advantageous allele spreading from the left will quickly be fixed on one side of the barrier ($x < 0$). Integrating Equation 2 over $x > 0$, assuming $q \approx 1$, and applying the boundary condition that $\partial p/\partial x = 1/B$ just to the right of a barrier at $x = 0$ shows that the total number of alleles on the other side ($x > 0$) will increase as:

$$\frac{\partial}{\partial t}\left(\int_0^\infty p\,dx\right) = \int_0^\infty \left(\frac{\sigma^2}{2}\frac{\partial^2 p}{\partial x^2} + Sp\right) dx$$

$$= -\frac{\sigma^2}{2B} + S\int_0^\infty p dx. \quad \text{(A1)}$$

Integrating over time,

$$\int_0^\infty p dx = \frac{\sigma^2}{2BS}(\exp(St) - 1) \quad \text{for } p \ll 1. \quad \text{(A2)}$$

Equation A2 accounts for the influx of alleles, and their subsequent increase. When $St \ll 1$, the influx becomes negligible, and the allele frequency approaches the Gaussian solution to Equation 2 with $q \approx 1$ and no influx, so that $(\partial p/\partial x) = 0$ at $x = 0$. Thus

$$p(x, t) = \frac{\sigma^2}{BS} \frac{\exp\left(St - \frac{x^2}{2\sigma^2 t}\right)}{\sqrt{2\pi\sigma^2 t}}. \quad \text{(A3)}$$

This is only valid for small p, and $St \ll 1$, but suggests that $p(0, t)$ will approach 1 after a time given by setting Equation A3 to 1 at $x = 0$; this time is an approximation to the delay caused by the barrier and is greater than the value of $ST = \log(\sqrt{\pi}\tilde{B}/2)$ given by BARTON (1979a) (see Figure 1A).

APPENDIX B

The rate of increase in variance of position can be calculated using the same method as for underdominance (BARTON 1979b). Let Fisher's solution to Equation 2 be $p_0(x - ct)$, where $c = \sigma\sqrt{2S}$. Denote deviations from this solution by $\omega(x - ct, t)$. These follow a linear diffrential equation that has one eigenfunction $(\Delta x \partial p_0/\partial x)$, which corresponds to a shift in position by Δx, and has eigenvalue zero. Since this is orthogonal to all the other eigenvalues, a perturbation $\epsilon(x)$ causes an eventual shift $\Delta x = \int \epsilon(x)(\partial p_0/\partial x)\,dx / \int (\partial p_0/\partial x)^2 dx$. The variance of perturbation ϵ is proportional to $p_0 q_0/2\rho$ in each generation, and so the rate of increase of $\mathrm{var}(\Delta x)$ is

$$\frac{\partial\, \mathrm{var}(\Delta x)}{\partial t} = \frac{\int_{-\infty}^{\infty} p_0 q_0 (\partial p_0/\partial x)^2 dx}{2\rho\left(\int_{-\infty}^{\infty} (\partial p_0/\partial x)^2 dx\right)^2}. \quad \text{(B1)}$$

Numerical solution of Equation 2 using the Runge-Kutta algorithm, followed by numerical integration of Equation B1, shows that this rate is $1.19\sigma/\rho\sqrt{2S}$.